Calibration of the Microwave Limb Sounder on the Upper Atmosphere Research Satellite!

Robert F. Jarnot, Joe W. Waters
Jet Propulsion Laboratory, MS 183-701
4800 Oak Grove Drive
Pasadena, CA 91109-8099 USA
T:818.354.5204, F:818.393.5065, EMail: jarnot@mlsrac.jpl.nasa.gov
T:818.354.3025, F:818.393.5065, EMail: joe@mlsrac.jpl.nasa.gov

Gordon E. Peckham
Physics Dept., Heriot-Watt University
Riccarton, Currie
Edinburgh EH14 4AS, Scotland
T:011.44.31.449.5111, EMail: peckham@abacus.phy.hw.ac.uk

ABSTRACT

This paper describes pre-launch radiometric aud spectral calibrations of the Microwave Limb Sounder (MLS) on the Upper Atmosphere. Research Satellite (UARS). Use of in-flight data for validation or refinement of calibration is described. The estimated uncertainty in calibrated radiance from prelaunch radiometric and spectral calibration data is better than 2% in most bands.

INTRODUCTION

The MLS onboard NASA's Upper Atmosphere Research Satellite is the first implementation of atmospheric limb sounding from space using microwaves. MLS was launched on September 12, 1991, becoming folly operational within 2 weeks of launch. The MLS is a passive instrument sensing thermal emission in 6 bands with radiometers centered near 63, 183 and 205 GHz. Primary measurements are stratospheric profiles of ClO, O_3, H_2O, temperature, and FOV tangent pressure which provides the pointing reference. Additional products include HNO_3, volcanically enhanced SO_2, upper tropospheric H_2O, and geopotential height. All data arc routinely analyzed and processed to produce daily maps of all retrieved quantities within 2 clays of data acquisition. This paper summarizes radiometric aud spectral calibrations. FOV calibrations arc described in a companion paper (Cofield, 1994). Complete details of all MLS calibrations are given in the MLS Calibration Report (Jarnot, et al, 1991).

INSTRUMENT

The MLS instrument is described in (Barath, et al, 1993), aud the measurement technique in (Waters, 1993). Table 1 lists its spectral bands and primary measurements.

TABLE 1 *MLS Spectral Bands and Primary Measurements*.

Radiometer	Band	LO Frequency	Primary Measurements
R1	1	63.28311 GHz	Pressure, Temperature
R2	2 aud 3	203.26686 GHz	ClO
	4		O_3
R3	5	184.77779 GHz	H_2O
	6		O_3

The MLS radiometers operate Doll-switched, aud its FOV step-scans the atmospheric limb every 65.536 s. Each limb scan consists of 32 minor frames of duration 2.048 s. The first ~1.8 s of each minor frame is used for signal integration aud digitization, the remaining time being available for movement of the antenna and/or switching mirror. All measurements are made simultaneously and continuously, and the bands are analyzed by 6 identical 15-channel filter banks, each of ~500 MHz bandwidth. Channel widths range progressively from 2 MHz at band center to 128 MHz at band edges, providing good resolution of spectral features as the FOV scans from ~90 km tangent height down to the mid-troposphere.

RADIOMETRIC CALIBRATION

MLS detectors are operated at a low rf power level to provide a linear relationship between channel output and input radiance, as illustrated in Figure 1

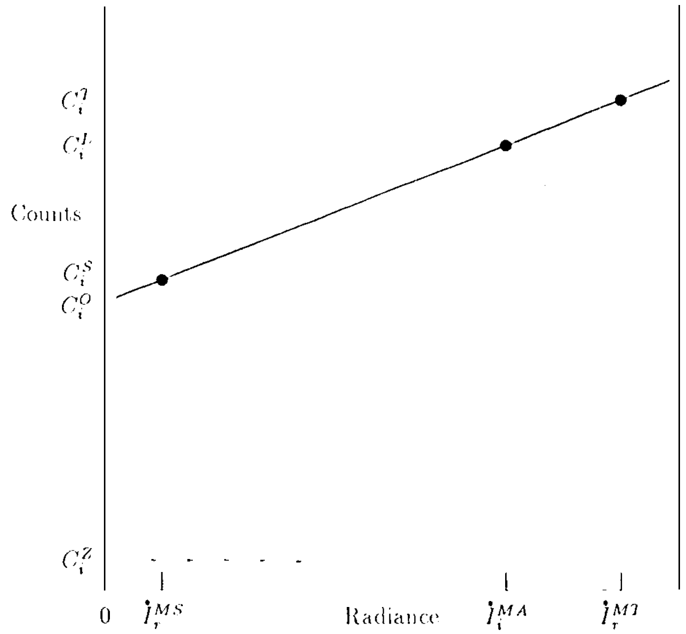

Figure 1: Linear relationship between counts and radiance.

A switching mirror simultaneously directs the FOVs of all radiometers to the limb, space or internal calibration target pelts The output, of channel i is given by:

$$C_i^X = g_i(\eta_r^X \dot{I}_r^X + (1-\eta_r^X)\dot{I}_r^{BX}) + C_i^O + C_i^N \qquad (1)$$

where, for the antenna:

- ρ_r^A is the ohmic loss
- η_r^A is the scattering loss
- $\dot I_r^{OA}$ is the radiation offset
- $\dot I_r^{SA}$ is the radiance scattered into the limb port

Pre-launch FOV calibrations provide ρ_r^A, η_r^A and $\dot I_r^{SA}$ for each radiometer.

In-flight radiometric calibration

Routine in-flight gain calibration provides g_i, and is performed every 65.536s by rotating the switching mirror so that the FOV of all radiometers is directed towards an internal ambient target for one minor frame, and to the space port for five minor frames.

An estimate of channel gain at the time of calibrations, g_i, is obtained from:

$$g_i = \frac{C_i^T - \langle C_i^S \rangle}{\eta_r^T \dot I_r^T - \eta_r^S \dot I_r^S + (1-\eta_r^T)\dot I_r^{BT} - (1-\eta_r^S)\dot I_r^{BS}}. \qquad (3)$$

The estimated space reference counts, $\langle C_i^S \rangle$, at the time of gain calibration views, is provided by quadratic interpolation over an 11 major frame window (55 space views) centered about the target frame. The estimate of gain at the time of each limb view, $\langle g_i \rangle$, is obtained by quadratic interpolation over an 11 major frame window as for the space view interpolation. Substituting (3) in (1) where X corresponds to the limb port gives:

$$\dot I_i^A = \frac{\left(\frac{C_i^L - \langle C_i^S \rangle}{\langle g_i \rangle} + \eta_r^S \dot I_r^S - (1-\eta_r^L)\dot I_r^{BL} + (1-\eta_r^S)\dot I_r^{BS}\right)}{\eta_r^L} \qquad (4)$$

The limb radiance obtained from (2) is:

$$\dot I_i^L = \frac{1}{\eta_r^A \rho_r^A}\left(\dot I_i^A - (1-\rho_r^A)\dot I_r^{OA} - (1-\eta_r^A)\rho_r^A \dot I_r^{SA}\right), \qquad (5)$$

where (4) is used for $\dot I_i^A$

Additional pre-launch radiometric calibration

In addition to determination of the calibration parameters above, internal target emissivity and end-to-end system linearity were measured. Target emissivity, 0.9998 or better in all bands, was determined by comparing the reflected power from a silver reference plate to that from the target using Gunn diodes as signal sources. The target is a wedge coated with iron-loaded epoxy pyramids, the pyramid size and spacing being chosen to avoid diffraction lobes in the frequency range covered by MLS. Target temperature is monitored by a network of 10 platinum resistance sensors embedded in the epoxy coating.

Linearity was measured by switching between the internal ambient calibration target and a similar external one attached to the space port. The external target included heaters to allow its temperature to be precisely controlled, and by measuring system output as a function of target temperatures, end-to-end system linearity was shown to be better than 0.1%. Independent tests on the filter banks indicate their non-linearity to be better than 0.05% over their full dynamic range.

Table 2 shows the scan pattern which has been used for the majority of the mission, and indicates the nominal tangent altitude of each limb view. The earth's oblateness is compensated by means of real-time commands from the spacecraft which allows target tangent heights to be tracked with daily variations of a few hundred meters rms.

TABLE 2. *Nominal in-flight Scan and Calibration Sequence*

Minor Frame	Step Angle	Motor Steps	Tangent Height/km	View Direction
0	0.0000	0	90.0	L
1	-0.1300	52	83.9	L
2	-0.1275	51	77.8	L
3	-0.1275	51	71.8	L
4	-0.1275	51	65.8	L
5	-0.1275	51	59.8	L
6	-0.1275	51	53.7	L
7	-0.0850	34	49.7	S
8	-0.0000	0	49.7	L
9	-0.0850	34	45.7	L
10	-0.0850	34	41.7	L
11	-0.0650	26	38.6	L
12	-0.0650	26	35.6	L
13	-0.0625	25	32.6	L
14	-0.0650	25	29.7	L
15	-0.0625	25	26.7	S
16	0.0000	0	26.7	L
17	-0.0500	20	24.3	L
18	-0.0300	12	22.9	L
19	-0.0300	12	21.5	L
20	-0.0300	12	20.0	L
21	-0.0300	12	18.7	L
22	-0.0300	12	17.3	L
23	-0.0450	18	15.1	S
24	0.0000	0	15.1	L
25	-0.0450	18	13.0	L
26	-0.0675	27	9.8	L
27	-0.0675	27	6.6	L
28	-0.0750	30	3.1	L
29	0.0000	0	3.1	S
30	Antenna retrace			T
31	Antenna retrace			S
	L = Limb, S = Space, T = Target.			

Diagnostics

Instrument performance is monitored once per orbit by reducing the gains of the signal chains to their minima, approximately 40 dB below their nominal settings, for 2 minor frames. This allows inference of system temperature, an indicator of front-end radiometer noise. In addition, the χ^2 statistic for the fit between interpolated and actual space view counts is routinely calculated for all channels by the ground processing software, providing a continuous measure of system stability.

SPECTRAL CALIBRATION

The response of radiometer channel i is proportional to the radiance $\dot I_i^X$ obtained by integrating the radiation incident on the switching mirror over angle and frequency with weighting functions $G_i(\nu, \theta, \phi)$ and $F_i(\nu)$ which describe the angular and frequency sensitivity of the receiver:

$$\dot I_i^X = \frac{1}{4\pi}\int_\nu\int_\Omega \dot I_u^X(\nu,\theta,\phi)\,F_i(\nu)\,G_i(\nu,\theta,\phi)\,d\Omega\,d\nu. \qquad (6)$$

$F_i(\nu)$ is normalised to unit area ($\int_\nu F_i(\nu)\,d\nu = 1$)

Channel shape
Considering only a single sideband, the calibrated signal radiance, $\bar{I}$, is given by:

$$\bar{I} = \frac{\int I(\nu)\, F(\nu) d\nu}{\int F(\nu) d\nu} \qquad (7)$$

where F is the end-to-end channel frequency response, I is the input radiance, and the integrals are evaluated over the full frequency range over which there is significant signal and instrument response. MLS spectrometers use LC filters in the outer (32 to 128 MHz width) channels, and SAW filters in the narrower center (2 to 16 MHz width) channels. The SAW filters have numerous ripples in their passbands, and all channels can have appreciable atmospheric radiance variation across their width, requiring all channels to be characterised with several hundred spectral points.

End-to-end sweeps using a synthesized fundamental source with a Cesium reference provided $F(\nu)$ in the broad outer channels of all bands, and in both sidebands of the radiometers. The source was coupled into the radiometer optically via a mirror on the space port. Channel gain and offset calibration were interleaved with signal measurement using the switching mirror, and source output was monitored continuously during the course of a sweep via power meters built into the transmitter output waveguide. All source and instrument operation, and data acquisition, were computer controlled. The narrow ($\leq$16 MHz) center channels were characterized by sweeping the spectrometers directly with a lower frequency synthesizer. The adequacy of these data was verified by comparison of channel shapes measured end-to-end and for the spectrometers alone for -32 MHz broad channels. Figure (2) shows examples of LC and SAW filter channel responses measured through the entire MLS signal path.

The fundamental source was also used to perform a broad (170 to 210 GHz) sweep to verify the lack of unwanted responses in this range for radiometers 2 and 3.

Relative sideband ratio
The differential radiometric calibration count, Δc_{cal}, is given approximately by:

$$\Delta c_{cal} = (I_{tgt} - I_{ref})(g_{sig} + g_{im}) \int F(\nu) d\nu \qquad (8)$$

where I_{tgt} and I_{ref} are the calibration and reference target radiances, g_{sig} and g_{im} are the signal and image frequency gains of the receiver, $F_i(\nu)$ the normalised frequency response of the receiver in channel i, and the integration is performed over all frequencies over which the instrument has a response.

For bands 2 through 6 of MLS the primary atmospheric signals of interest occur in one sideband, and an atmospheric signal $I(\nu)$ in the signal sideband generates a signal count, Δc_{sig}, where:

$$\Delta c_{sig} = g_{sig} \int I(\nu) \quad F(\nu) d\nu \qquad (9)$$

and the inferred Level 1 signal radiance, I_{sig}, is given by:

$$I_{sig} = \frac{\Delta c_{sig}}{\Delta c_{cal}} (T_{tgt} - T_{ref}) \qquad (10)$$

or equivalently

$$I_{sig} = \left(\frac{g_{sig}}{g_{sig} + g_{im}}\right) \frac{\int I(\nu) F(\nu) d\nu}{\int F(\nu) d\nu} \qquad (11)$$

We may rewrite the factor which contains the sideband gains as $\frac{1}{1+r}$, where r is the ratio of image to signal sideband response.

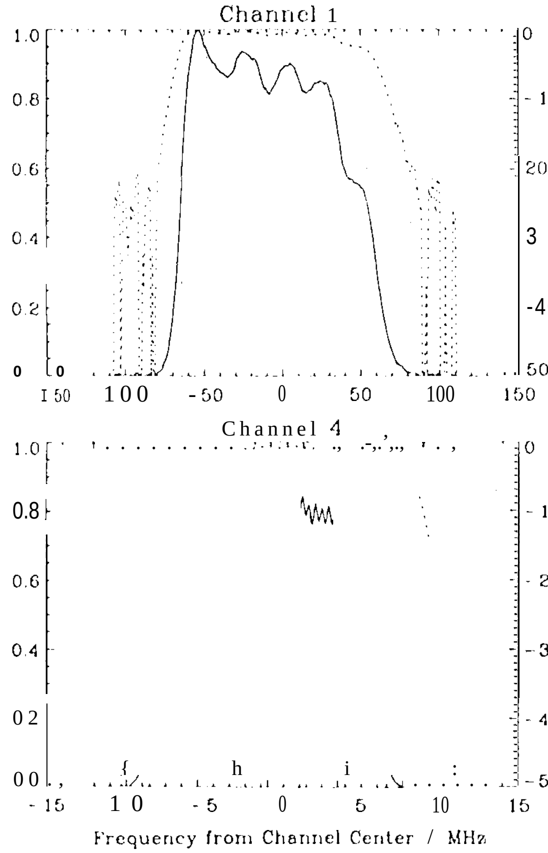

Figure 2: Measured LC (upper) and SAW filter channel responses. Vertical axes are linear (solid line) and logarithmic (dashed line) responses.

Thus, when $r \sim 1$, an uncertainty of a factor δ in knowledge of r leads to an uncertainty of a factor of approximately $\frac{\delta}{2}$ in the interpretation of the signal radiance.

Sideband calibration
Relative sideband responses of the radiometers were measured using an external scanning Fabry-Pérot interferometer as a tuneable filter while switching between views to ambient and LN_2 cooled calibration targets. A similar pair of targets viewed directly provided periodic gain calibration. The computer controlling MLS also operated the mechanisms for switching between views of the four targets, and for varying the Fabry-Pérot grid spacing. Grid spacing was stepped over the ranges 10 to 13 and 30 to 33 mm in steps of 0.01 mm to allow all channels in all bands of the radiometers 2 and 3 to be swept through at least four orders of the Fabry-Pérot. Results from the sweep of a 128 MHz wide channel in band 4 is shown in Figure 3, and Figure 4 shows measured (crosses) relative sideband response in bands 2 through 4.

Systematic errors in the differences between measured and calculated Fabry-Pérot transmissions were used to estimate the errors in calibrated radiance, amounting to ~0.6% in bands 2 to 4, and ~2% in band 5. The corresponding uncertainty in band 6 was estimated at 4% in band 6, due to limitations imposed by the narrow (<200 MHz) spacing of the signal and image sidebands

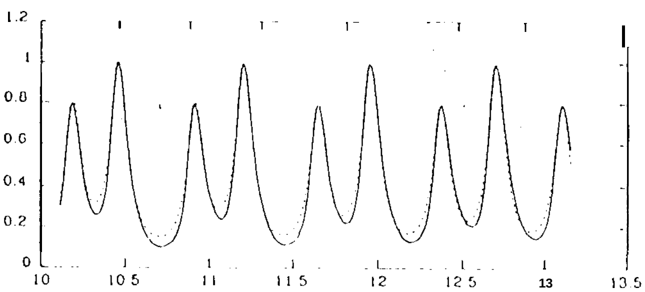

Figure 3: An example of MLS sideband sweep data. Vertical axis is relative transmission, horizontal axis is grid separation in mm. Dashed lines are calculated response, after fitting to the measurements.

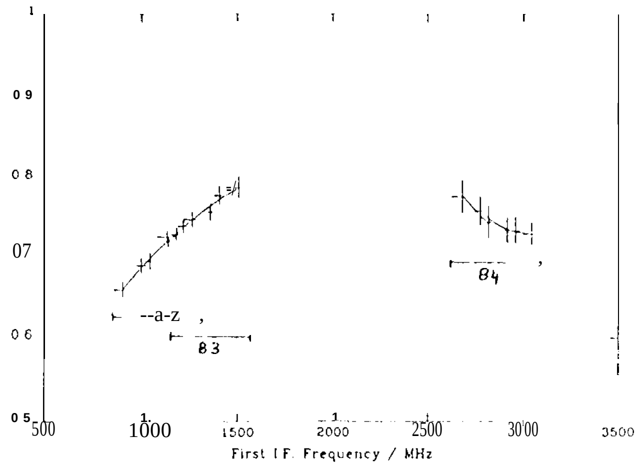

Figure 4: MLS relative sideband response in bands 2 through 4. Crosses are measurements, curve is fit used in data processing.

FIELD-OF-VIEW CALIBRATION

FOV calibration includes:

- Antenna fal-field FOV, necessary for relating observed antenna radiance to actual limb radiance.
- Radiometer-to-radiometer boresight angle differences, since the 63 GHz radiometer provides pointing data for all bands.
- Determination of antenna scattering, loss and emissivity in all bands.
- Estimation of the baffle transmissions for the three orifices viewed by the switching mirror,

These topics, together with the use of in-flight data for calibration refinement, are discussed in a companion paper (*op cit*).

IN-ORBIT DATA

The calibration philosophy for MLS was that all calibrations be performed before launch, with validation and possible minor refinement, from in-orbit data.

Temperature gradients in the material of the internal calibration target were anticipated from the results of ground tests. These were characterised early in the mission with tests which exposed the surface of the target to space via the limb port for varying lengths of time, and then observing target radiance for several minor frames with the cooling path 10 space blocked by the switching mirror. A skin depth (and hence band) dependent relaxation of target radiance was observed as the target material regained thermal equilibrium, but at Such a low level (<0.5"(; in any band) as to impart negligible error in radiometric gain calibration.

The atmospheric signals in each sideband of bands 4, 5 and [i become optically thick ? at different tangent altitudes, and these data provide a test of sideband ratio calibration. By choosing data sets for which the atmosphere was close to isothermal, it was found that sideband calibrations appeared to be Collect, but that B3 benefited slightly from a revised analysis of the pre-launch calibration data.

STABILITY

Accurate pre-launch calibration is only useful if long-term system stability is such that drifts in instrument characteristics over the mission lifetime do not add significant additional error. The antenna and radiometer optics were tested by measuring beam patterns before and after vibration testing. All frequency sources within the instrument are phase locked to a highly stable quartz master oscillator, Long-term stability of the spectrometer filters was verified by performing life tests at elevated operating temperatures, and by vibration tests.

Relative sideband ratio was found to be insensitive to temperature and local oscillator drive levels for the variations expected over mission life. Sensitivity to mixer bias was found to be significant. DC mixer bias is controlled directly by ground command, and RF bias is controlled indirectly through ground control of multiplier bias voltage, allowing compensation for ageing of the Gunn diode oscillators. MLS mixers are operated in flight at their ground test bias levels.

RESULTS

A comprehensive, accurate and high-resolution set of engineering data are measured every minute to monitor instrument operation. These data, together with derived performance parameters (e.g. channel gain and stability), have been closely monitored for the duration of the mission, and no significant change or trend has been observed in any parameter or characteristic, apart from the failure of the 183 GHz mixer after 18 months, its nominal operationallife.

Radiance residuals, the differences between observed spectra and those expected from the retrieved data, are calculated routinely to monitor the performance of the retrieval software. These are highly sensitive to errors in calibration parameters such as channel position, shape and sideband ratio, overall radiometric calibration, and FOV parameters such as band-to-band boresight knowledge. Study of these residuals, and results from the MLS data validation) program, indicate no significant errors in pre-launch instrument calibrations, and no discernable change in any calibration parameter

CONCLUSIONS

Radiometric calibration accuracy appears to be better than ~1% in all bands, with similar errors arising in most bands **from** spectroscopic calibration.

The MLS has demonstrated the viability of microwave limb sounding from low Earth orbit, having so far provided over two